

Performance of Column with Upper-Anchored Grouted Corrugated Duct Connections Under Load

Jie Zhang ¹, Chenxi Fu ^{2*}, Yuanhong Fu ³ and Siyuan Li ²

¹ Nanjing Highway Development Center, Nanjing 210014, Jiangsu Province, China;

² China Design Group Co., Ltd., Nanjing 210014, Jiangsu Province, China;

³ Liuhe District Highway Development Center of Nanjing City, Nanjing 211500, Jiangsu Province, China.

* Correspondence: 274292857@qq.com

Abstract: The core goal of the prefabricated construction of urban prestressed concrete bridges is to improve structural performance and construction efficiency. To improve the construction convenience and load-bearing performance of the connection between precast columns and pile caps, a novel connection structure for upper-anchored grouted corrugated ducts is proposed in this study. By comparing the pushover damage process of the integral casting column, the column connected by the grouting sleeve and the column connected by the upper-anchored grouted corrugated duct, the effects of the column height and the axial compression ratio on the performance of the column connected by the grouted corrugated duct were analyzed. Research results indicate that columns with upper-anchored grouted corrugated ducts exhibit superior static performance and ductility, with horizontal load-carrying capacities 23% greater than those of integrally cast columns and ductility performances 98% greater than those of integrally cast columns. Additionally, the primary concrete damage areas of these structures are farther from the bottom joint interface, featuring a wider distribution range of damaged areas and higher plastic hinge heights. When designing connections for columns with upper-anchored grouted corrugated ducts, controlling the elastic curvature ratio at section locations (sections with enlarged dimensions and sections at the base of columns) to be no less than 1.8 is recommended.

Citation: Zhang, J.; Fu, C.; Fu, Y.; Li, S. Performance of Column with Upper-Anchored Grouted Corrugated Duct Connections Under Load. *Prestress Technology* 2025, 1, 01-13. <https://doi.org/10.59238/j.pt.2025.01.001>

Received: 19/12/2024

Accepted: 10/01/2025

Published: 30/03/2025

Publisher's Note: Prestress technology stays neutral with regard to jurisdictional claims in published maps and institutional affiliations.



Copyright: © 2025 by the authors. Submitted for possible open access publication under the terms and conditions of the Creative Commons Attribution (CC BY) license (<https://creativecommons.org/licenses/by/4.0/>).

Keywords: precast columns; upper-anchored grouted corrugated duct connection method; pushover analysis

1 Introduction

The construction of bridge columns for long urban and highway prestressed concrete bridges is highly suitable for standardized, factory-based, and prefabricated construction methods. Utilizing precast assembled bridge columns not only significantly reduces the onsite working time and shortens the construction period but also improves the quality of column construction, minimizes impacts on traffic and the environment, and increases economic and social benefits. Therefore, research on the connection structures and mechanical performance of precast assembled bridge columns has become a hot topic both domestically and internationally [1-3].

At present, the commonly used methods for connecting prefabricated columns and pile caps in China include the Prestressed Tendon connection method, the Grouted Sleeve connection method, and the Grouted Corrugated Duct Connection Method. The grouted sleeve connection method is a type of mechanical reinforcement connection that can be divided into top-anchored and bottom-anchored types (Figure 1). Owing to the simpler prefabrication and grouting process of the top-anchored connection method, it is more commonly used in actual projects. Studies by Haber et al. [4] and Tazarv et al. [5] through scaled quasistatic tests revealed that the failure mode and ultimate load of columns connected by grouted sleeves are close to those of cast-in-place columns, but the ductility performance is

25% to 40% lower than that of cast-in-place columns. Additionally, the grouted sleeve connection method has stringent requirements for construction precision and grouting quality, leading to higher costs. The influence of sleeve size also increases the thickness of the concrete cover, limiting the performance of longitudinal reinforcement, which restricts its widespread application.

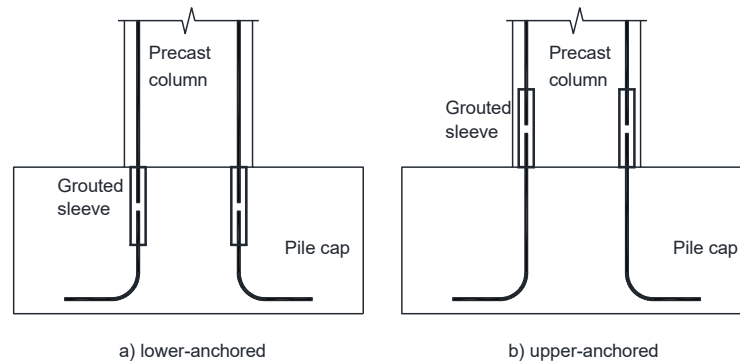


Figure 1 Grouted sleeve connection method

In contrast, the grouted corrugated duct connection method is more suitable for connecting precast bent caps to columns, but its application in connecting columns to pile caps is relatively rare, with existing applications predominantly utilizing lower-anchored structures (Figure 2). This is because grouted corrugated ducts allow for larger construction tolerances and thus require more space for placement. Implementing an upper-anchored structure would make it difficult to ensure adequate spacing between the corrugated ducts. However, in lower-anchored structures, corrugated ducts are typically embedded within the pile cap, necessitating longer rebar anchorage lengths; this increases the complexity of prefabricating, transporting, and installing columns.

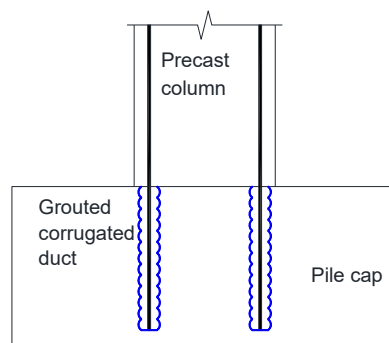


Figure 2 Grouted corrugated duct connection method

In research on lower-anchored grouted corrugated duct connections, Pang et al. [6] demonstrated through scaled experiments that the load–deflection curves of precast columns connected with corrugated ducts are similar to those of integral cast-in-place columns. Restrepo et al. [7] reported that the drift ratio of precast assembled columns connected with grouted corrugated ducts is 80% of that of integral cast-in-place columns. Tazarv et al. [5] reported that fully plastic hinges can form at grouted corrugated duct connections, achieving an ultimate drift ratio of up to 12%. In their seismic quasistatic tests, Jiang et al. [8] noted that damage to precast columns is concentrated mainly at the column base joints and plastic hinge zones, with slightly lower ductility than integral cast-in-place columns but similar seismic performance. Both domestic and international experimental studies have shown that properly designed and constructed grouted corrugated duct-connected columns exhibit

strengths and ductility performances close to those of integral cast-in-place columns, indicating promising development prospects [8-10].

This paper proposes a new upper-anchored grouted metal corrugated duct connection scheme in which corrugated ducts are placed inside columns, offering both construction convenience and economic benefits while enhancing mechanical performance. Pushover numerical analysis is used to compare the mechanical performance and failure modes of three schemes—integral cast-in-place, grout sleeve connections, and grouted corrugated duct connections—and the influences of parameters such as the column height and axial compression ratio on the performance of upper-anchored grouted corrugated duct connections are discussed. This provides a reference for optimizing the design of precast assembled bridge columns.

2 Connection Structure of Upper-Anchored Grouted Corrugated Ducts

2.1 Structural Arrangement

The structure of the upper-anchored grouted corrugated duct connection between the column and the pile cap is shown in Figure 3. In this design, the corrugated ducts are preembedded at the bottom end of the precast columns, whereas the connecting rebars are preembedded in the pile cap. During construction, the connecting reinforcement from the pile cap are inserted into the preembedded grouted corrugated ducts within the columns, and anchoring is achieved through grouting. To enhance the connection performance, a section with an enlarged cross-section is designed at the bottom of the precast column. The functions of this enlarged section include (1) ensuring that the standard section cover thickness does not need to be thickened, thereby improving the effectiveness of the longitudinal reinforcement in the column; (2) providing sufficient cover thickness for the corrugated ducts; and (3) enhancing the strength of the potential plastic hinge zone at the bottom of the column, improving the cracking pattern and ultimate failure mode of the column.

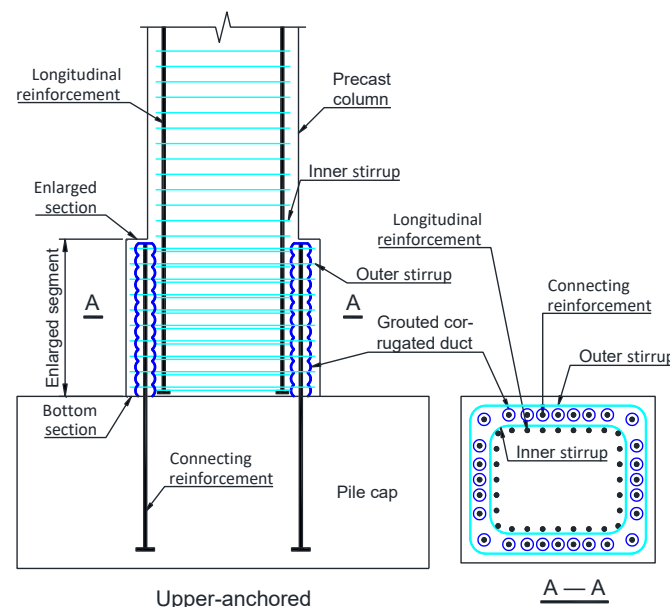


Figure 3 Upper-anchored grouted corrugated duct connection method

The longitudinal reinforcement of the columns is continuously arranged down to the bottom of the enlarged section, with threaded anchors at the ends of the longitudinal reinforcements to ensure their anchoring performance. The connecting reinforcement from the pile cap are placed on the outer side of the column's

longitudinal reinforcements and are aligned one-to-one with them. The number and total area of the connecting reinforcements in the pile cap must not be less than those of the longitudinal reinforcements within the columns. The longitudinal reinforcements of the columns and the connecting reinforcements of the pile cap form a lap splice region within the enlarged section of the column, effectively transferring loads.

Within the enlarged section of the column, both the inner and outer layers of the stirrups are arranged. The inner layer of stirrups is located on the outer side of the column's longitudinal reinforcements, whereas the outer layer of stirrups is positioned on the outer side of the pile cap connecting reinforcements. The stirrup ratio of the outer layer should not be less than that of the inner layer to increase the strength of the core concrete, improve the ductility of the component, and prevent reinforcement buckling. The joint between the column and the pile cap is filled with a mortar bedding layer of 20 to 30 mm thickness.

This study is based on a renovation and expansion project of a certain section of Provincial Highway 126 in Jiangsu Province, where the details of the upper-anchored grouted corrugated duct connection were designed. The longitudinal reinforcements of the columns and the connecting reinforcements of the pile cap utilize HRB400-grade steel reinforcements with a diameter of 36 mm. The selected corrugated ducts are metal ducts with a diameter of 103 mm and a length of 970 mm, meeting the anchoring requirements for the reinforcements.

2.2 Anchorage Length of the Grouting Corrugated Duct

In the upper-anchored connection structure, the anchoring length of the corrugated duct is a critical design parameter that determines the height of the enlarged section of the column. To determine the anchoring length of grouted metal corrugated ducts, the US National Cooperative Highway Research Program (NCHRP) 12-105 [11] synthesized data from 35 sets of pull-out tests and proposed a recommended formula that considers both reinforcement anchorage failure and corrugated duct anchorage failure:

$$l_d = \max \left(\frac{0.68f_s d_b}{\sqrt{fg}}, \frac{2.25f_s d_b^2}{d_a \sqrt{f'_c}} \right) \tag{1}$$

where:

l_d is the anchoring length (in inches);

f'_c is the standard value of the concrete compressive strength (in psi);

f_s is the stress in the reinforcement (in psi), which is taken as the larger value between 1.5 times the yield strength and the ultimate strength;

f is the compressive strength of the grout (in psi);

d_a is the inner diameter of the corrugated duct (in inch);

d_b is the diameter of the longitudinal reinforcement (in inch).

The NCHRP 12-105 project also specifies that the diameter of the corrugated duct should not be less than 2.75 times the diameter of the reinforcement, and the spacing between adjacent corrugated ducts must be greater than either 50 mm or 1.3 times the maximum aggregate size of the concrete, whichever is larger.

According to the Chinese standard "The grouting corrugated steel ducts for rebar anchorage" (T/CECS 10098—2020), the minimum effective anchoring length of the reinforcement inside the corrugated duct should be 24 times the diameter of the reinforcement, and the difference between the minimum inner diameter of the corrugated duct and the diameter of the reinforcement should not be less than 35 mm. Taking the conventional substructure column design in China as an example, using C40 concrete and HRB400-grade steel reinforcement, with the grout compressive strength set at 100 MPa, the calculated minimum anchorage length of the duct is 24

times the diameter of the reinforcement, which is consistent with the recommended results from the NCHRP 12-105 project.

3 Structural Finite Element Model

To investigate the full-range mechanical performance of precast concrete column–pile cap structures connected by upper-anchored grouted corrugated ducts, a pushover analysis was conducted via ABAQUS finite element software for three different connection methods: monolithic casting, grouted sleeve connection, and grouted corrugated duct connection. The reference model was a monolithic cast-in-place column with cross-sectional dimensions of 1.4 m × 1.4 m and a total height of 5.5 m. The longitudinal reinforcement of the column had a diameter of 36 mm, and the stirrups had a diameter of 12 mm. For the precast assembled column, a 20 mm thick high-strength mortar layer was placed between the precast column and the pile cap.

The nonlinear behavior of concrete was modeled using the Concrete Damaged Plasticity (CDP) model, with its uniaxial constitutive relationship based on the “Code for Design of Concrete Structures” (GB 50010—2010). The concrete strength grade of the precast column was C40, and the corresponding stress–strain curves for the concrete under tension and compression are shown in Figure 4.

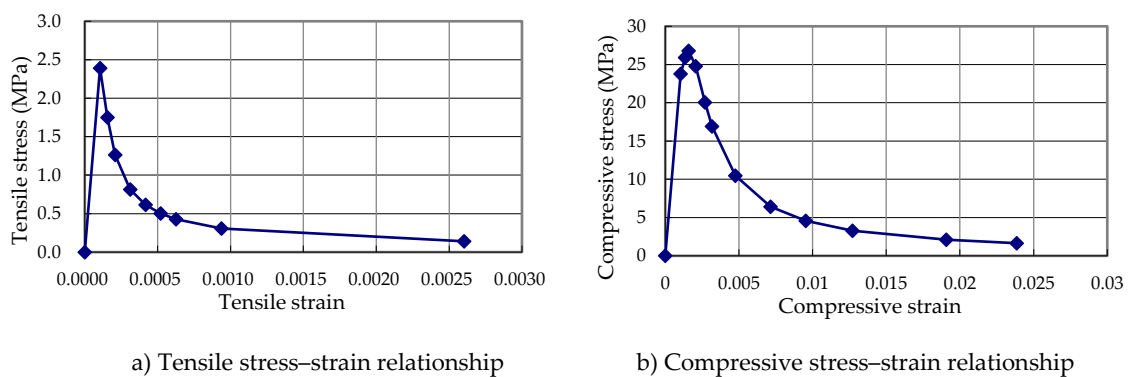
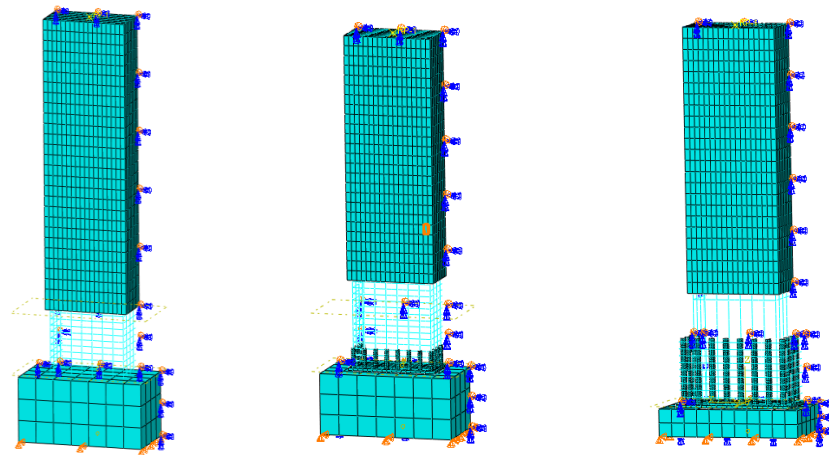


Figure 4 Tensile and compressive damage stress–strain curves of the concrete

The material model for the high-strength mortar layer was based on the constitutive relationship of C80 concrete. Since the joint in the assembled column disrupted the continuity of the concrete, a reduction factor of 0.6 was applied to the tensile strength of the high-strength mortar to simplify the analysis and reflect the structural cracking characteristics.

The ordinary reinforcement, sleeves, and metal corrugated ducts were modeled via an ideal elastic–plastic material model. The ordinary reinforcement (HRB400) had an elastic modulus of 200 GPa, a yield strength of 400 MPa, and an ultimate strength of 600 MPa. The sleeve had an elastic modulus of 200 GPa, a yield strength of 400 MPa, and a thickness of 20 mm. The metal corrugated duct had an elastic modulus of 200 GPa, a yield strength of 275 MPa, an ultimate strength of 440 MPa, and a thickness of 2 mm.

The finite element model is shown in Figure 5. Owing to the symmetry of the model, only half of the structure was analyzed. The column, pile cap, and high-strength mortar layer were modeled via 3D 8-node reduced integration elements (C3D8R). The longitudinal and stirrup reinforcements were modeled via 2-node truss elements (T3D2). The grouted sleeve and metal corrugated duct were modeled using shell elements (S4R). The mesh size ranged from 10 to 20 cm. The precast column and pile cap were connected via tie constraints, and the longitudinal and stirrup reinforcements were embedded into the concrete via embedded constraints.



a) Monolithic cast-in-place b) Grouted sleeve connection c) Grouted corrugated duct connection

Figure 5 Finite element model of the column

The loading of the model was divided into two steps: (1) Axial loading: A constant axial load of 4500 kN was applied at the top of column; (2) horizontal displacement loading: A horizontal displacement was applied at the top of column, with a maximum displacement of 360 mm. The Abaqus implicit algorithm was used to simulate the nonlinear mechanical behavior accurately.

4 Performance Comparison of the Three Connection Schemes

4.1 Shear Force–Displacement Curves at the Bottom of Column

The bottom shear force–top displacement curves and characteristic loads of the three types of columns are shown in Figure 6 and Table 1. The load–displacement curves of the three columns exhibits similar patterns. The definitions of the characteristic loads are as follows:

- (1) Cracking load: The load at which plastic tensile strain appears in the concrete of the column, indicating the onset of cracking.
- (2) Yield load: The load at which the longitudinal reinforcement on the tension side yields.
- (3) Peak load: The maximum load value in the load–displacement curve.
- (4) Ultimate failure load: This load is assumed to be 85% of the peak load, corresponding to the ultimate state of the component in the pushover curve.

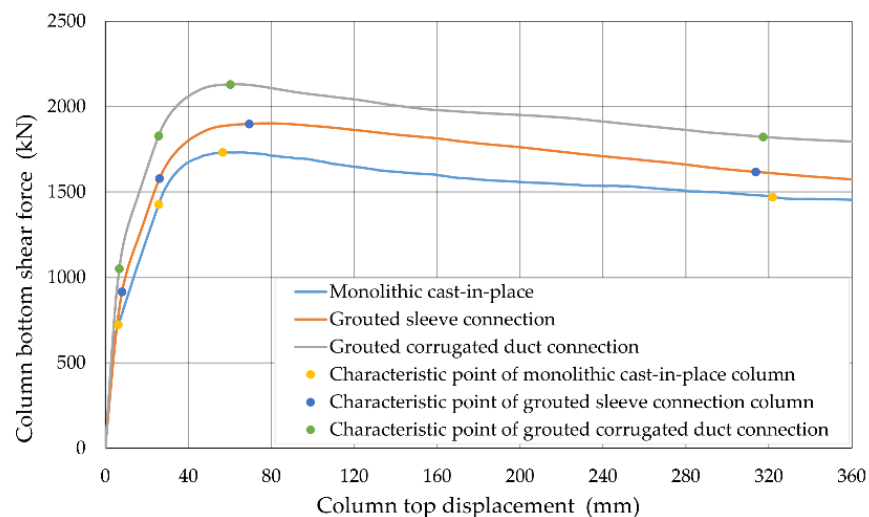


Figure 6 Load–displacement curves of columns

In terms of the horizontal load-bearing capacity, the load-bearing capacity of the column with grouted corrugated duct connection is 1.23 times greater than that of the monolithic cast-in-place column, which is significantly greater than that of the monolithic cast-in-place column. This performance improvement stems from the following factors:

- (1) The increased cross-sectional dimensions at the bottom of column lead to a greater effective height, significantly enhancing the cracking load and ultimate load.
- (2) Although the enlarged section is a standard cross-section, its ultimate load-bearing capacity is relatively high due to the smaller shear span ratio.

Combining these effects, the column with the grouted corrugated duct connection exhibited the highest peak load and superior horizontal load-bearing capacity.

To evaluate the deformation capacity of each column type, the actual load–displacement curves were idealized into elastic–perfectly plastic load–displacement curves. The equivalent method was determined according to the “Specifications for Seismic Design of Highway Bridges” (JTGT 2231-01–2020). The equivalent yield load and its corresponding displacement are listed in Table 1. The displacement ductility coefficient of the columns is defined as the ratio of the ultimate displacement to the equivalent yield displacement. The displacement ductility coefficients of all three column types exceed 10.0, indicating excellent plastic ductility performance. Among them, the ductility coefficients of the columns with grouted sleeve connections and grouted corrugated duct connections are 95% and 98% of those of monolithic cast-in-place columns, respectively.

Table 1 Load and displacement characteristics of columns

Category	Yield load (kN)	Equivalent yield load (kN)	Peak load (kN)	Failure load (kN)	Peak load ratio
Monolithic cast-in-place column	1,427.1	1,613.6	1,731.4	1,470.0	1.0
Grouted sleeve connection column	1,577.6	1,801.1	1,898.7	1,617.3	1.1
Grouted corrugated duct column	1,829.0	2,091.1	2,129.7	1,822.5	1.2
Category	Yield displacement (mm)	Equivalent yield displacement (mm)	Peak displacement (mm)	Ultimate displacement (mm)	Ductility coefficient
Monolithic cast-in-place column	25.7	29.1	56.7	321.8	11.1
Grouted sleeve connection column	26.2	29.9	69.5	313.7	10.5
Grouted corrugated duct column	25.7	29.3	60.2	317.3	10.8

4.2 Concrete Normal Stress

The bottom of the column and the enlarged section (or 1.0 m above the base) were selected as control sections. Figure 7 shows the normal stress–displacement curves of the three types of columns. The figure shows that on the tension side edge of the columns, concrete cracking occurs at relatively low displacements for all three column types, leading to the concrete being out of work. Additionally, the cracking load difference between the bottom and the enlarged section (or 1 m above the base) of the same column is minimal; this is because the column height is significant, and the distance between the two control sections is relatively small.

On the compression side edge of the columns, the stress development in the monolithic cast-in-place column and the grouted sleeve connection column is similar. In both cases, the concrete at the bottom section of the column first reaches its ultimate compressive strength. At the Section 1 m above the base, the ultimate compressive strength of the concrete is not reached even when the column top

reaches its ultimate displacement. Compared with the monolithic cast-in-place column, the stress unloading at the base of the grouted sleeve connection column is slower, which is attributed to the increased stiffness of the bottom section of the column due to the grouted sleeve. In contrast, the development of compressive stress in grouted corrugated duct connection columns differs significantly from that in the other two column types. The ultimate compressive strength of the concrete in the grouted corrugated duct connection column first appears at the section change location, after which the stress gradually decreases. During the stress reduction in the enlarged section, the compressive stress at the base increases slightly, but the concrete at the bottom section of the column does not reach its ultimate compressive strength even when the column top reaches its ultimate displacement.

In summary, the control section for the monolithic cast-in-place column and the grouted sleeve connection column is located at the base, where the plastic hinge forms. For the grouted corrugated duct connection column, the control section is located at the enlarged section. During the material softening phase, significant stress redistribution occurs at the base and the enlarged section, ultimately forming a plastic hinge centered at the enlarged section.

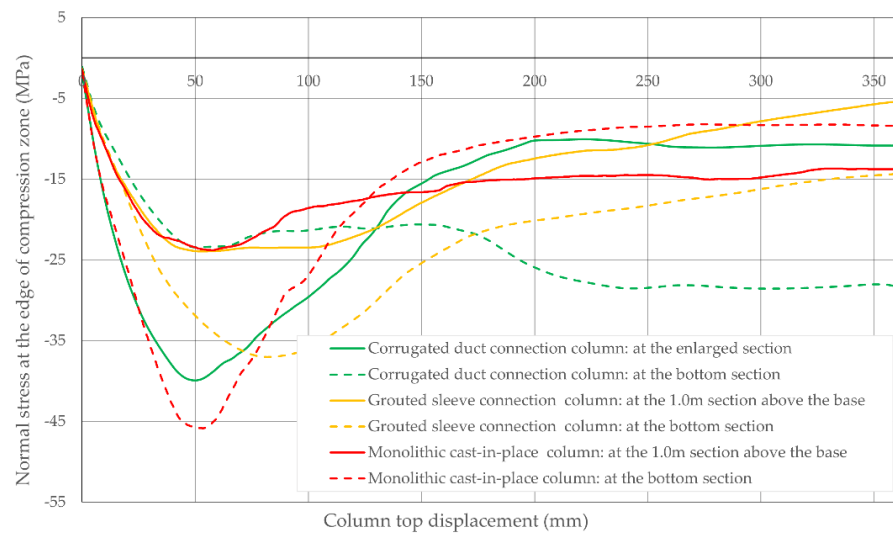
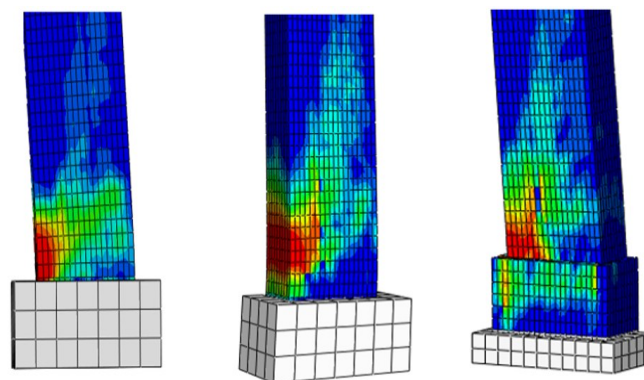


Figure 7 Concrete stress—displacement curves of columns

4.3 Failure Modes

Figure 8 shows the contour plots of the concrete compressive damage factor for the three column types at the ultimate displacement state of the column top. In this state, both the tensile and compressive reinforcements in the columns reached their yield strength, but the stirrups did not yield.



a) Monolithic cast-in-place b) Grouted sleeve connection c) Grouted corrugated duct connection

Figure 8 Concrete compressive damage factor contour plots

The distribution curves of damage energy dissipation along the height of the columns at the same displacement state are shown in Figure 9. The damage energy dissipation of the columns is the sum of the damage energy dissipation of the elements in the same layer of the finite element model. The figure shows that the distribution of concrete damage energy dissipation along the height indicates significant differences in the location and extent of plastic hinge distribution among the three column types. For monolithic cast-in-place columns, the damage to the concrete is concentrated at the base, with the smallest plastic hinge distribution height. For the grouted sleeve connection column, the sleeve significantly influences the distribution of damage energy dissipation. The damage energy dissipation increases sharply at the top of the sleeve, forming a single peak that develops symmetrically upward and downward, resulting in concentrated plastic damage and a moderate plastic hinge distribution height. For the grouted corrugated duct connection column, the distribution of damage energy dissipation is somewhat similar to that of the grouted sleeve connection column, also forming a single peak. However, the peak is located at the enlarged section, developing upward to the standard section of the column and downward to the bottom section of the column. Owing to the influence of structural dimensions, the upward development is more pronounced than the downward development, the distribution range of plastic damage is larger, and the plastic hinge height is the highest.

In summary, although the load–deflection curves of the three column types are similar, their ultimate failure mechanisms and modes differ. These differences must be considered in the structural design and verification of columns.

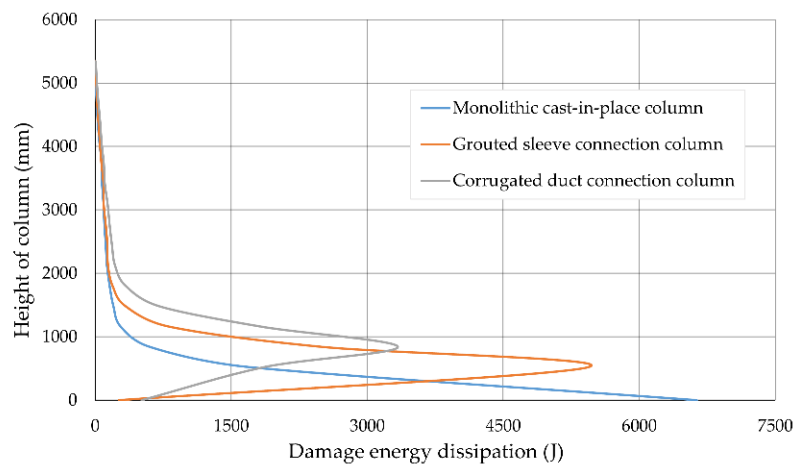


Figure 9 Damage energy dissipation of columns

5 Parameter Analysis

5.1 Influence of Column Height (Elastic Curvature Ratio) on Grouted Corrugated Duct Connection Columns

When the column height varies while the cross-sectional dimensions remain similar, the two control sections (the enlarged section and the bottom section) exhibit different elastic curvatures. The distribution of elastic curvature significantly influences the bending failure mode of a section. Additionally, since the dimensions of the enlarged section are primarily controlled by construction requirements, the elastic curvature ratio between the two key sections also reflects the influence of the shear span ratio on the mechanical performance. The elastic curvature ratio β between the bottom section of the standard column segment and the bottom section of the column can be expressed as:

$$\beta = \frac{(H-H_1)I_{c0}}{H \cdot I_c} \tag{2}$$

where:

I_c is the moment of inertia of the standard column segment;

I_{c0} is the moment of inertia of the bottom section;

H is the total height of the column;

H_1 is the height of the enlarged section column segment.

The relationships between the column height and elastic curvature ratio are shown in Table 2. In the analysis model, the structural form and reinforcement of the enlarged section column segment remain the same, whereas only the length of the standard column segment is varied.

Table 2 Column heights and elastic curvature ratios

Column height (m)	2.50	3.50	4.50	5.50	6.50	8.50
Elastic curvature ratio	1.37	1.63	1.77	1.86	1.93	2.01

The load–displacement curves for columns of different heights are shown in Figure 10. As the column height increases, the yield load and peak load of the column decrease significantly, whereas the yield displacement and peak displacement increase notably. This indicates that as the column height increases, the deformation capacity of the column improves, whereas the horizontal load-bearing capacity gradually decreases. When the column height exceeds 4.5 m (i.e., the elastic curvature ratio exceeds 1.77), the precast assembled columns exhibit good ductility, with a slow reduction in post-peak stiffness and strong deformation capacity. However, when the column height is less than 4.5 m, the post-peak strength of the assembled columns decreases rapidly, the ultimate displacement is small, and the displacement ductility coefficient is low, making them unsuitable for design as ductile components.

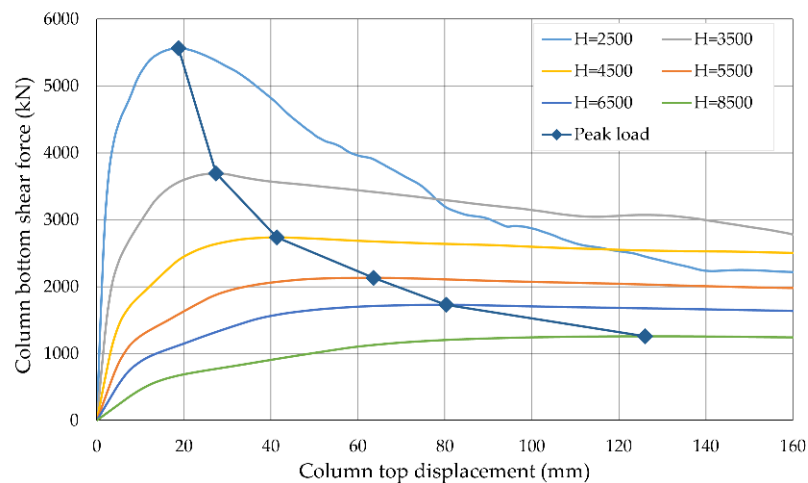


Figure 10 Load–displacement curves for different column heights

The distribution of concrete damage energy dissipation along the column height at the peak load for grouted corrugated duct connection columns of different heights is shown in Figure 11. For shorter columns (2.5 m and 3.5 m), the damage distribution is relatively wide, covering both the enlarged section and the standard column segment, with peak plastic damage occurring at the bottom of the enlarged section, indicating that the failure control section is at the bottom section. For taller columns (height > 4.5 m, elastic curvature ratio > 1.77), the plastic damage to the concrete is concentrated, with the peak located at the enlarged section, and the damage distribution width at the base is relatively small, indicating that the failure control section is at the enlarged section and that a plastic hinge forms at the enlarged section.

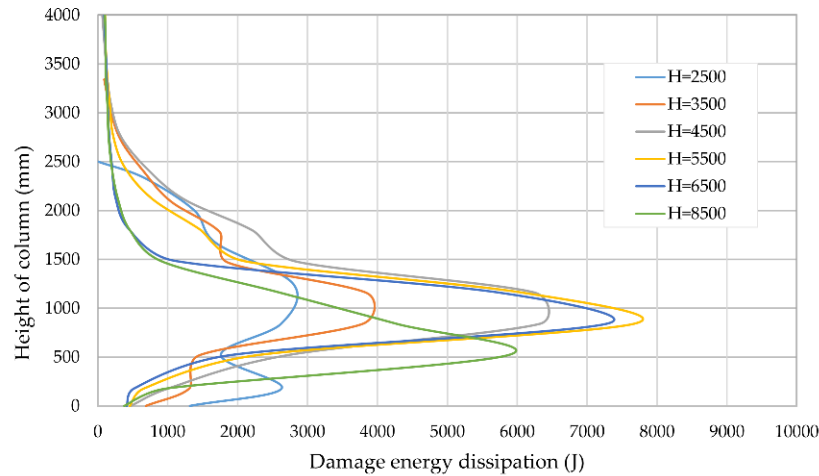


Figure 11 Damage energy dissipation distributions for different column heights

In summary, to ensure that the upper-anchored grouted corrugated duct connection columns exhibit good ductility and that the plastic hinge forms at the control section (enlarged section) within the column, the elastic curvature ratio between the two control sections (enlarged section and bottom section) should be greater than 1.8 during the structural design of the column.

5.2 Influence of the Axial Compression Ratio

The axial compression ratio under dead loading is an important parameter affecting the seismic performance of columns. The load–displacement curves for grouted corrugated duct connection columns under different axial compression ratios are shown in Figure 12. As the axial compression ratio increases, the deformation capacity of the column decreases, which has a significant adverse effect on the ductility design of the column. In seismic fortification zones, the axial compression ratio of bridge columns is generally not greater than 0.2, with 0.1 being commonly used. The influence of the axial compression ratio on the performance of upper-anchored precast assembled columns is similar to that of conventional columns.

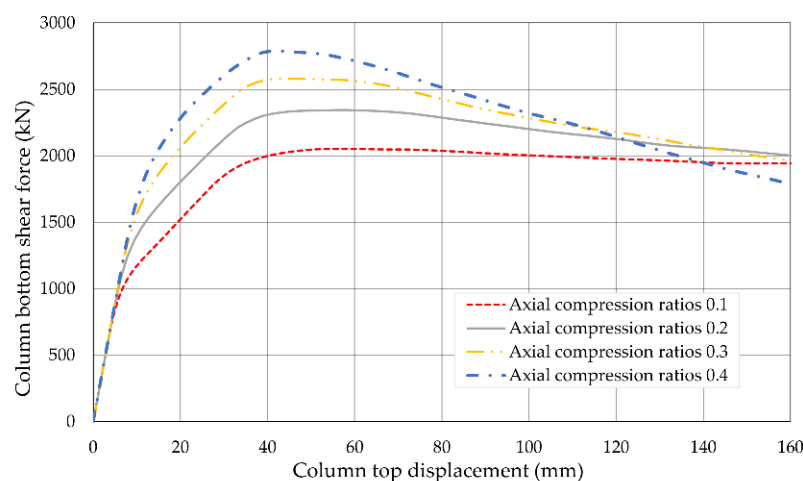


Figure 12 Influence of the axial compression ratio on the load–displacement curves

The distribution of damage energy dissipation along the column height under the same displacement for grouted corrugated duct connection columns under different axial compression ratios is shown in Figure 13. The overall trend of the damage energy dissipation distribution is similar for columns with different axial

compression ratios. However, under the same column top displacement, columns with higher axial compression ratios exhibit higher peaks and wider distributions of concrete plastic damage. This finding indicates that the axial compression ratio does not affect the location of the plastic hinge center but increases the distribution range of the plastic hinge. As the axial compression ratio increases, the peak concrete plastic damage also increases, potentially leading to earlier ultimate failure of the column and limiting the ductility of the column.

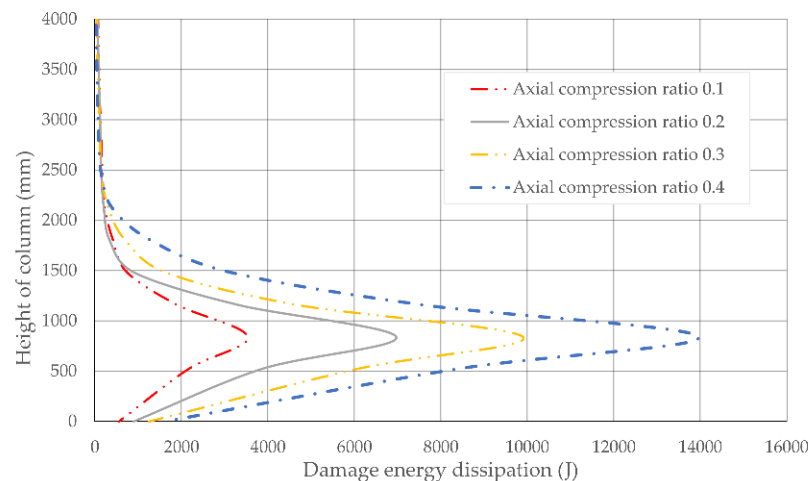


Figure 13 Influence of the axial compression ratio on the damage energy dissipation distribution

6 Conclusions

- (1) The upper-anchored grouted corrugated duct connection method for precast columns offers significant economic and construction advantages, effectively improving the static and ductility performance of precast assembled columns.
- (2) Pushover analysis revealed that the horizontal load-bearing capacity of upper-anchored grouted corrugated duct connection columns is significantly greater than that of monolithic cast-in-place columns, whereas the load-bearing capacity of grouted sleeve connection columns is similar to that of monolithic cast-in-place columns. The location and extent of plastic hinge distribution differ significantly among the three column types: concrete damage in monolithic cast-in-place columns and grouted sleeve connection columns is concentrated at the bottom section of columns, whereas plastic damage in upper-anchored corrugated duct connection columns is more widely distributed, centered at the enlarged section, and presents a greater plastic hinge height.
- (3) In the design of upper-anchored grouted corrugated duct connection columns, the elastic curvature ratio between the two control sections (enlarged section and bottom section) should be no less than 1.8 to ensure good ductility and mechanical performance.

To further validate the reliability of the numerical analysis and the seismic performance of the connection, static and dynamic tests are planned to explore the actual mechanical behavior of upper-anchored grouted corrugated duct connection columns under complex loading conditions. Additionally, research on the long-term performance of the connection will be conducted, focusing on the durability of the joints and the degradation of grout material properties, providing more comprehensive design guidelines for practical engineering applications.

Conflict of interest: All the authors disclosed no relevant relationships.

Data availability statement: The data that support the findings of this study are available from the corresponding author, Fu, upon reasonable request.

References

1. Tazarv, M.; Shrestha, G.; Saiidi, M.S. State-of-the-Art Review and Design of Grouted Duct Connections for Precast Bridge Columns. *Structures* **2021**, *30*, 895-909, doi:10.1016/j.istruc.2020.12.091.
2. Wang, J.Q.; Shen, Y.; Li, G.P.; Chen, M.; Fan, C.X. Quasi-Full-Scale Experimental Study on Bridge Precast Concrete Columns under Static Loading. *J Bridge Eng* **2021**, *26*, doi:10.1061/(Asce)Be.1943-5592.0001725.
3. GE, J.; YAN, X.; WANG, Z. Seismic Performance of Prefabricated Assembled Pier with Grouted Sleeve and Prestressed Reinforcements. *Journal of Traffic and Transportation Engineering* **2018**, *18*, 42-52, doi:10.3969/j.issn.1671-1637.2018.02.005.
4. Haber, Z.B.; Saiidi, M.S.; Sanders, D.H. Seismic Performance of Precast Columns with Mechanically Spliced Column-Footing Connections. *Aci Struct J* **2014**, *111*, 639-650.
5. Tazarv, M.; Saiidi, M.S. Low-Damage Precast Columns for Accelerated Bridge Construction in High Seismic Zones. *J Bridge Eng* **2016**, *21*, doi:10.1061/(Asce)Be.1943-5592.0000806.
6. K., P.J.B.; P., S.K.; L., C.; etc. *Rapidly Constructible Large-Bar Precast Bridge-Bent Seismic Connection*; University of Washington: Seattle, America, 2008.
7. Restrepo, J.I.; Tobolski, M.J.; Matsumoto, E.E. Development of a Precast Bent Cap System for Seismic Regions. *NCHRP Report* **2011**, doi:10.17226/14484.
8. Jiang, H.; Wang, Z.; Shen, J. Anti-seismic Performance Testing of Prefabricate Assembly Pillars Connected with Grouting Metal Corrugated Pipe. *Structural Engineers* **2016**, *32*, 132-138.
9. Wang, Z.; Wei, Z.; Wei, H.; Wang, H. Influences of Precast Segmental Connector Forms on Seismic Performance of Bridge Pier. *China Journal of Highway and Transport* **2017**, *30*, 74-80, doi:10.3969/j.issn.1006-3897.2017.05.010.
10. Jia, J.; Guo, Y.; Song, N.; Zhu, Y.; Du, X.; Geng, L. Seismic Testing of Precast RC Bridge Pier Columns Anchored by Grouted Corrugated Ducts. *China Journal of Highway and Transport* **2018**, *31*, 211-220, doi:10.3969/j.issn.1001-7372.2018.12.021.
11. Saiidi, M.S.; Mehraein, M.; Shrestha, G.; Jordan, E.; Itani, A. *Proposed AASHTO Seismic Specifications for ABC Column Connections*; Transportation Research Board: Washington, 2020.

AUTHOR BIOGRAPHIES

	<p>Jie Zhang M.E., Senior Engineer. Working at Nanjing Highway Development Center. Research Direction: Highway Construction and Maintenance Management. Email: 37615279@qq.com</p>		<p>Chenxi Fu M.E., Professor Engineer. Working at China Design Group Co., Ltd. Research Direction: Design and Development of Bridge Engineering. Email: 274292857@qq.com</p>
	<p>Yuanhong Fu M.E., Engineer. Working at Liuhe District Highway Development Center of Nanjing City. Research Direction: Highway Construction and Maintenance Management. Email: 783644994@qq.com</p>		<p>Siyuan Li M.E., Engineer. Working at China Design Group Co., Ltd. Research Direction: Design and Development of Bridge Engineering. Email: 519800185@qq.com</p>